Eur. Phys. J. B **61**, 131–139 (2008)
DOI: 10.1140/epjb/e2008-00063-7

THE EUROPEAN PHYSICAL JOURNAL B

First principles study of structural, magnetic and electronic properties of half-metallic CrO_2 under pressure

V. Srivastava[1], M. Rajagopalan[2,a], and S.P. Sanyal[1]

[1] Department of Physics, Barkatullah University, Bhopal 462026, India
[2] Department of Physics, Anna University, Chennai 600 025, India

Received 29 August 2007 / Received in final form 28 November 2007
Published online 16 February 2008 –

Abstract. A first-principles tight-binding linear muffin tin orbital (TB-LMTO) method within the local-density approximation is used to calculate the total energy, lattice parameter, bulk modulus, magnetic moment, density of states and energy band structures of half-metallic CrO_2 at ambient as well as at high pressure. The magnetic and structural stabilities are determined from the total energy calculations. From the present study we predict a magnetic transition from ferromagnetic (FM) state to a non-magnetic (NM) state at 65 GPa, which is of second order in nature. We also observe from our calculations that CrO_2 is more stable in tetragonal phase (rutile-type) at ambient conditions and undergoes a transition to an orthorhombic structure ($CaCl_2$-type) at 9.6 GPa, which is in good agreement with the experimental results. We predict a second structural phase transition from $CaCl_2$- to fluorite-type structure at 89.6 GPa with a volume collapse of 7.3%, which is yet to be confirmed experimentally. Interestingly, CrO_2 shows half metallicity under ambient conditions. After the first structural phase transition from tetragonal to orthorhombic, half metallicity has been retained in CrO_2 and it vanishes at a pressure of 41.6 GPa. Ferromagnetism is quenched at a pressure of 65 GPa.

PACS. 71.15.Mb Density functional theory, local density approximation, gradient and other corrections – 71.15.Nc Total energy and cohesive energy calculations – 75.50.-y Studies of specific magnetic materials

1 Introduction

There has been a renewed interest in 3*d*-transition metal oxides (TMO) during the last decade. As the changes in *d* bandwidth are controlled by pressure, the high-pressure studies of TMO have been regarded as a useful way to understand their basic properties. Insulator-metal transition, magnetic moment collapse and electron topological transitions are some of the phenomenon, which may occur under high pressure. In addition, structural phase transitions induced by pressure are also a striking subject. Out of the numerous TMO, Chromium dioxide (CrO_2) has received a renewed attention not only due to its practical importance in technology of spintronics, tunneling magneto-resistance devices, magnetic heads and magnetic field sensors [1–3] but also for its distinct transport, optical, electronic and structural properties [4–9]. Under ambient conditions CrO_2 crystallizes in rutile-type structure (space group $P4_2/mnm$). Extensive theoretical and experimental studies on pressure induced structural and electronic properties of several transition metal dioxides (TMDO) have been reported in literature [10–14]. Among these oxides, Chromium dioxide is the only ferromagnetic (FM) compound with a Curie temperature of ≈390 K, which in addition, shows 'half-metallic' behavior with a magnetic moment of $2\mu_B$ per Cr atom. In its half-metallic (HM) behavior, one spin species is metallic and other is semiconducting resulting in a typical transport property i.e. it shows anomalously large resistivity but still metallic at high temperature [14,15]. It has been found in various electronic studies [4,5] of CrO_2 that density of states (DOS) at the Fermi level varies from 0.69 states/Ry.f.u. [5] to 2.34 states/Ry.f.u. [4]. Moreover, earlier studies [4,16,17] on band structure calculations at ambient conditions are diverse with the HM picture of α-CrO_2. The electronic properties predicted by Matar et al. [9,17] are in good agreement with that of the Schwarz [15]. On the other hand, Kulatov et al. [4] found a gap for both majority and minority spins, which is inconsistent with that of the Schwarz [15]. Nikolaev et al. [16] computed a magnetic moment of $1.772\mu_B$ per Cr atom which is in conflict with the HM (must be $2\mu_B$) picture of α-CrO_2. On the other hand, it is revealed from the literature that experimentally [18–21], half-metallicity in CrO_2 has been extensively studied and fairly understood. For example Keizer et al. [20] have injected new excitement into the field of half-metals by reporting the existence of a spin triplet super current through the strong ferromagnet

[a] e-mail: mraja1948@yahoo.co.in

CrO_2. However, correlations in the theoretical and experimental studies of half-metallic ferromagnetic CrO_2 are discussed by Dedkov et al. [22].

So far as the structural, magnetic and electronic properties of α-CrO_2 at high-pressure are concerned, one recent experimental study is presented by Maddox et al. [8] using angle-resolved synchrotron X-ray diffraction study. According to their observations, rutile-type CrO_2 transforms to $CaCl_2$-type (space group, $Pnnm$) structure under a pressure of 12.8 GPa without any discontinuity in volume. Such type of transformation (rutile to $CaCl_2$-type) under pressure in other TMDOs [10–13] is a common phenomenon. However, their electronic role to structural constancy is noteworthy in TMOs at high pressure. They are the prototypical examples of strongly correlated electron systems. Pressure induced electronic study of MnO [23] also concludes to metallisation, electronic valence transformation in several TMO [24,25] are the some examples, where electrons play crucial role. As far as the theoretical electronic studies of CrO_2 at high-pressure are concerned, there has been no report till now up to our knowledge. Under the application of pressure the disappearance of magnetism and half-metallicity is yet to be explored in details, however, we undertook this problem and solved up to some extent.

Structural phase transition, collapse of magnetic moment and half-metallicity are reported for a number of rutile-type TMO compounds [8–13,26,27]. Since CrO_2 also belongs to the same family namely, rutile-type, we like to know whether this also fall into the same category. This is the main motivation of the present work and this is achieved by performing both non-spin- and spin-polarised electronic band structure calculations using first principles tight binding linear muffin tin orbital (TB-LMTO) method at ambient as well as at high pressures. The organization of the paper is as follows: Section 2 describes the computational details of the TB-LMTO method. In Section 3 potentially interesting results are discussed. The corresponding Sections 3.1 and 3.2 deal with the results of the ground state, magnetic properties, and electronic band structures in three structures, respectively. Finally in Section 4, we summarize the results.

2 Method of calculation

The total energy, band structure and density of states for CrO_2 are calculated in nonmagnetic (NM) and ferromagnetic (FM) states, similar to our previous work [28] using TB-LMTO method [29,30] within the local-density approximation (LDA) [31]. von-Barth and Hedin [32] parameterization scheme had been used for exchange correlation potential. α-CrO_2 crystallizes in the rutile-type structure (space group, $P4_2/mnm$) and magnetically stable in FM state. The rutile structure has a simple tetragonal Bravais lattice with two formula units per unit cell [5]. In FM ground state, chromium and oxygen atoms are located at positions: Cr : (0, 0, 0) and O : $(u, u, 0)$ with $u = 0.305$. The structure of the high-pressure phase is β-CrO_2 with positions at Cr : (0, 0, 0) and O : $(u, v, 0)$ ($u = 0.299$ and $v = 0.272$) while in fluorite structure these atoms are positioned at Cr : (0, 0, 0) and O : (0.25, 0.25, 0.25). Total energy (per formula unit) was calculated for CrO_2 in these three structures. The Wigner-Seitz sphere was chosen in such a way that the sphere boundary potential is minimum and the charge flow between the atoms is in accordance with the electro-negativity criteria. The **E** and **k** convergence were also checked. The tetrahedron method [33] of Brillouin zone integration had been used to calculate the total density of states. The total energy was computed by reducing the volume from 1.05 V_0 to 0.70 V_0, where V_0 is the equilibrium cell volume. The calculated total energy was fitted to Birch equation of state [34] to obtain the pressure volume relation. The pressure is obtained by taking volume derivative of the total energy. The bulk modulus $B = -V_0 dP/dV$ is also calculated from $P - V$ relation. It is well known that the LMTO method gives accurate results for closely packed structures. Since the structures under consideration are loosely packed, empty spheres are introduced to make them densely packed with out breaking the crystal symmetry.

3 Result and discussion

3.1 Structural properties

The structural properties of half-metallic ferromagnetic (HMF) CrO_2 will be discussed at ambient and high pressures in this section. We have calculated total energies of CrO_2 in rutile-, $CaCl_2$- and CaF_2-type structures by using first principles TB-LMTO method. A picture containing the three structures, is shown in Figure 1. The Cr atoms form a body-centred tetragonal lattice and are surrounded by a slightly distorted octahedron of oxygen atoms (Fig. 1a). An orthorhombic $CaCl_2$-type structure is shown in Figure 1b, while Figure 1c shows a cubic fluorite type structure of CrO_2. Figure 2 shows the variation of total energies (per formula unit) with relative volume in NM and FM states for rutile structure. From our calculation we find that CrO_2 is more stable in the FM state than in NM state. The equilibrium cell volume in FM state is estimated to be 55.53 Å^3 and the corresponding lattice parameter $a = 4.384$ Å and $c = 2.889$ Å with $c/a = 0.659$, which can be compared well to the experimentally [8] obtained value of a is 4.421 Å and c is 2.916 Å. The calculated error in the lattice parameter is 0.8%. The Muffin Tin radii (R_{MT}) used in the present calculation for Cr, O, E and E1 (empty spheres) as 2.308, 1.878, 1.807 and 1.649 a.u., respectively. From Figure 2 we infer a magnetic to nonmagnetic transition in α-CrO_2 at a pressure of 65 GPa without any volume collapse, which can be seen from Figure 3, which depicts a $P - V$ relationship. For want of experimental results we are unable to compare the present prediction. However, most of the oxides of Fe, Mn, Co and Ni show magnetic collapsing at very high pressure [26]. From the present study we find that the contributions to the magnetic moment come entirely from Cr atom rather than O atom. At ambient pressure the calculated magnetic moment is 2.0 μ_B/Cr, which is in good agreement

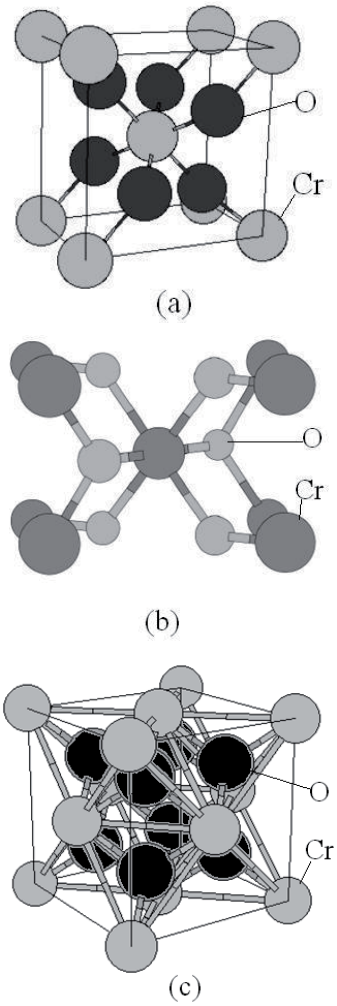

Fig. 1. Illustration of crystal structures of CrO_2 in (a) rutile-type (b) $CaCl_2$-type (d) CaF_2-type.

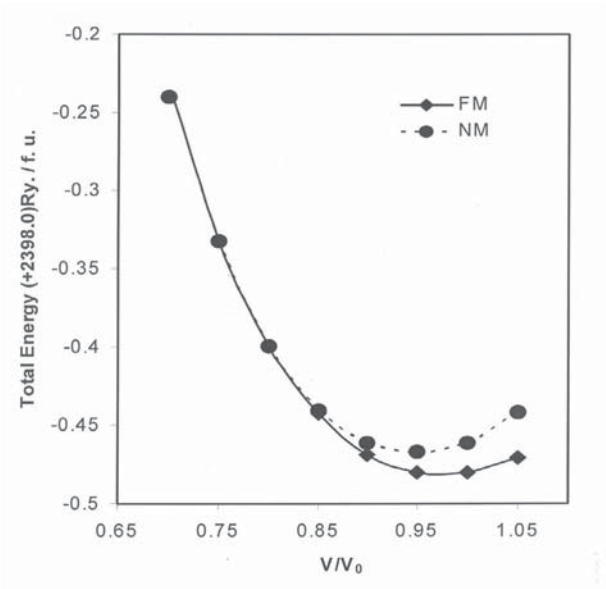

Fig. 2. Variation of total energy with relative volume in ferromagnetic and non-magnetic states of rutile-type CrO_2.

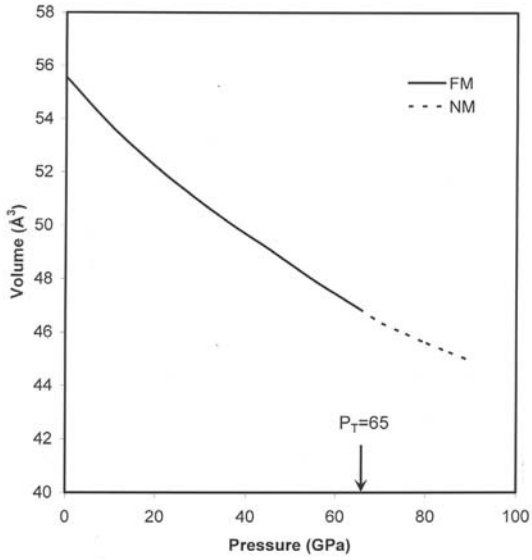

Fig. 3. Pressure-volume relation for rutile-type CrO_2.

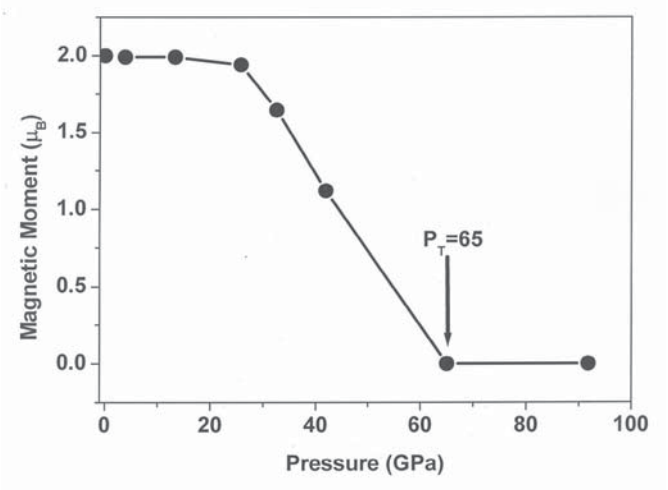

Fig. 4. Magnetic moment (in Bohr magnetons (μ_B)) of ferromagnetic CrO_2 in rutile structure as function of pressure.

with the others theoretical and experimental value [5,9]. The variation of magnetic moment under pressure is given in Figure 4. It is clear from the figure that magnetic moment of Cr atom decreases as pressure increases and at a pressure of 65 GPa the magnetic moment becomes zero, which results into a magnetic to a nonmagnetic transition.

The total energies (per formula unit) in rutile-, $CaCl_2$- and CaF_2-type structures are calculated and shown in Figure 5. The difference in energy between rutile- and $CaCl_2$-type structures is very close. So we have plotted the total energies for the above two phases only and given in Figure 6 separately. From the figure one can easily observe that CrO_2 undergoes a structural phase transition from rutile- to $CaCl_2$-type structure at 9.6 GPa with 1.6% volume collapse, which is in good agreement with the experimentally [8] observed value of 12.8 GPa without volume discontinuity. The total energies are fitted to Birch

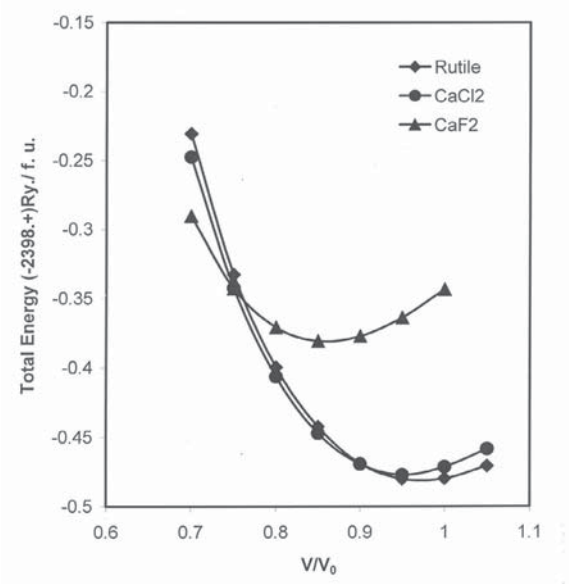

Fig. 5. Total (per formula unit) energy variation of CrO_2 in different structures.

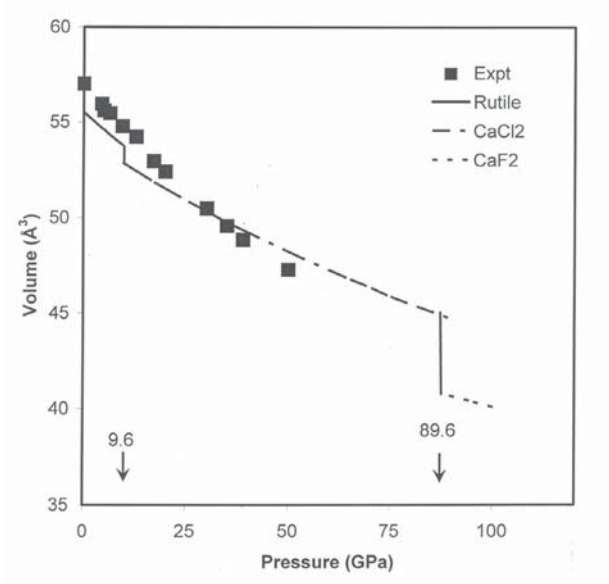

Fig. 7. Equation of states for CrO_2. Experimental points (■) are taken from reference [8].

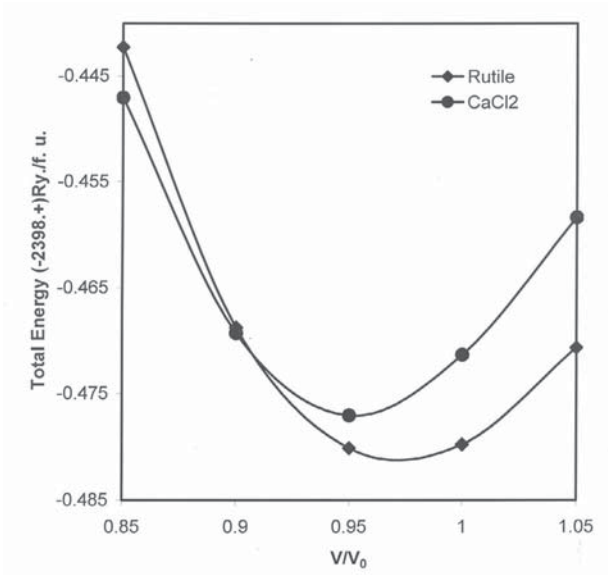

Fig. 6. A close look of total (per formula unit) energy variation of CrO_2 in rutile and $CaCl_2$-type structures.

equation of state to obtain the pressure volume relation and it is given in Figure 7. The bulk modulus at ambient pressure (B_0) is 143.3 GPa with the value of B_0' as 4.47. In the high-pressure phase (i.e. $CaCl_2$) the bulk modulus is found to be 193 GPa. From the present study we predict that CrO_2 also undergoes yet another structural phase transition from $CaCl_2$ to CaF_2-type structure at 89.6 GPa with a volume collapse of 7.3%. We predict the bulk modulus to be 338.2 GPa with 4.334 Å as lattice parameter in CaF_2 phase, which is yet to be confirmed experimentally. Other rutile-structured dioxides [28] like RuO_2, SnO_2 and PbO_2 also transform to fluorite-type phase via $CaCl_2$-type phase. Therefore, high-pressure experimental studies are needed to verify our present results.

3.2 Electronic properties

We have performed spin polarized electronic structure calculations of CrO_2 in the rutile-type and $CaCl_2$-type structures only. The band structures (BS) and density of states (DOS) at ambient conditions are calculated and shown in Figures 8–10. Figure 8 depicts the band structure of minority spins, while band structure for majority spins in rutile phase, is shown in Figure 9. In Figure 8 the lowest lying bands are due to *s*-like states of oxygen and the Fermi level (shown by dotted line), lies between the oxygen *p*-like and chromium *d*-like states showing its semiconducting nature. In Figure 9 mixing of Cr-*d* states and O-*p* states near E_f can be seen showing its metallic nature. Figure 10 shows the DOS for both spins, which confirms the half metallic character of CrO_2, which is in excellent agreement with the others reported [5–7,15] work. Due to the ferromagnetic decoupling, one of the spin subbands (generally the majority-spin or up-spin subband) is metallic, whereas the Fermi level falls into a gap of the other (down-spin) subband. One can understand the reason of half-metallicity in CrO_2 as, in majority-band case the interaction of Cr-*d* states and O-*p* states leads to a mutual repulsion so that the O-*p* states are pushed to energies above the Fermi level. These O-*p* states connect with lower states and are responsible for metallic character of the majority-band structure. Since the Cr-*d* levels are polarized above the Fermi level in the minority-spin direction, the same interaction of O-*p* and Cr-*d* states presses the O-*p* levels below the Fermi level opens a gap, and produces semiconducting behaviour. Half metals are the extreme case of strong ferromagnets (or saturated Hubbard ferromagnets), where

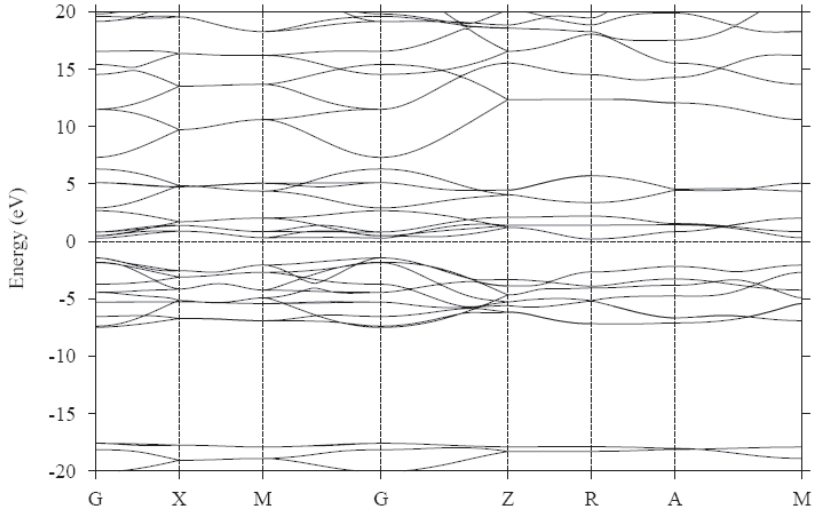

Fig. 8. Band structure for minority spins in ferromagnetic CrO_2 at ambient pressure in rutile structure.

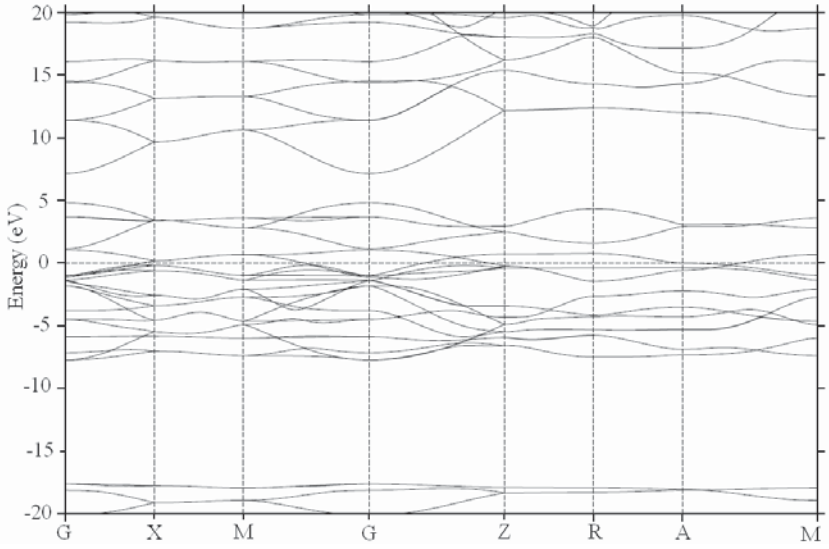

Fig. 9. Band structure for majority spins in ferromagnetic CrO_2 at ambient pressure in rutile structure.

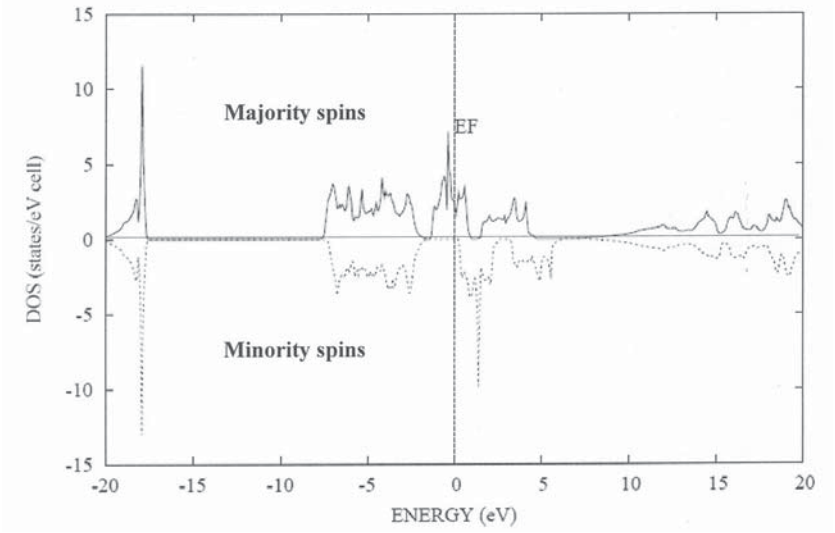

Fig. 10. Total (per formula unit) density of states for majority and minority spins in ferromagnetic CrO_2 at ambient pressure in rutile structure.

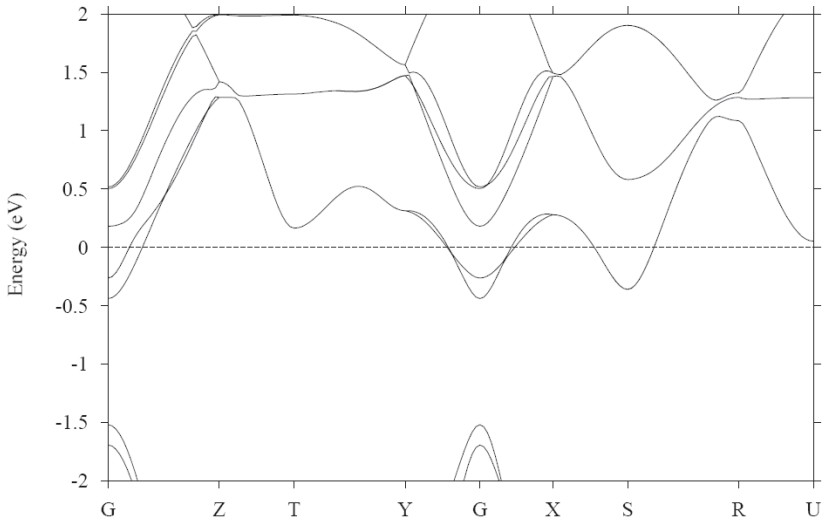

Fig. 11. Band structure for minority spins of ferromagnetic CrO_2 at $P = 9.6$ GPa in $CaCl_2$-type structure.

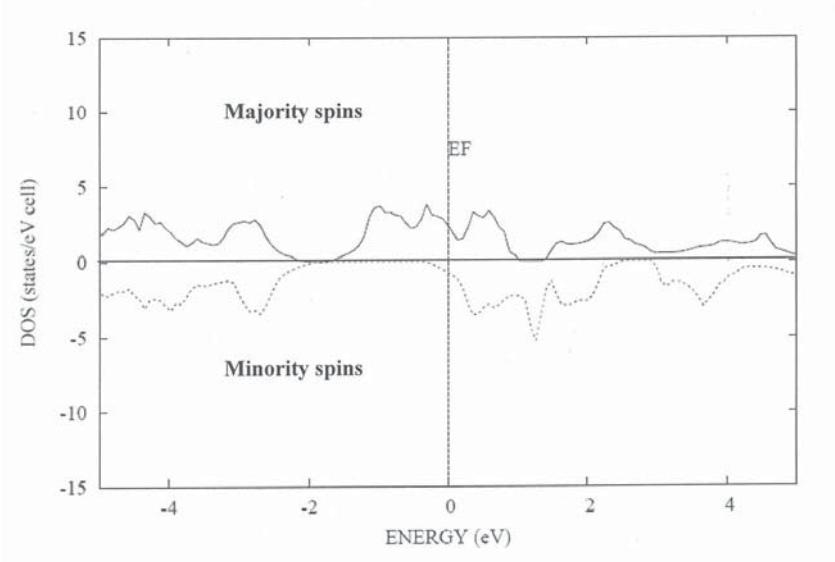

Fig. 12. Total (per formula unit) DOS for HMF CrO_2 at $P = 9.6$ GPa in $CaCl_2$-type structure.

not only $3d$ electrons are fully polarized, but also other (sp) down-spin bands do not cross the Fermi level. These conditions can be met in manganese compounds particularly, as the large intra-atomic exchange results in the full alignment of local spins and thus in the exclusion of down-spin electrons from the $3d$ shell [35]. Very recently, half-metallic and FM to NM transition in manganese pnictides have been reported [36]. From the present calculations, for half-metallic state the magnetic moment is found to be 2.0 μ_B/Cr, which is in good agreement with the values reported by Schwarz [14] and Lewis [5]. The calculated density of majority states at Fermi level is 2.30 states/eV/f.u., which is in good agreement with the others results [4].

As discussed above, CrO_2 undergoes a structural phase transition from rutile to a $CaCl_2$-type structure at a pressure of 9.6 GPa. The band structure and the density of states are obtained and given in Figures 11 and 12, respectively. The overall profile is found to be similar to that of the rutile structure. But we noticed a small difference in the DOS for the minority spin channel where the d-like band of Cr is slightly moved into E_f, which is due to broadening of the d-like band under pressure. Nevertheless, CrO_2 shows semiconducting in all directions (Z, T, Y, X, R, U in Fig. 11) except a few (G, S in Fig. 11). At this pressure, the computed magnetic moment is found to be 1.833μ_B/Cr.

As pressure increases half metallicity of the compound decreases, which can be understood as minority spins also show metallic character (semi conductivity deceases), while majority spins remain metallic. The minority band gap deceases with decrease in volume, which is due to the exchange interaction between the majority and minority spins [37]. The decrease in volume results in strong bonding, which will delocalize the d-electrons, thereby reduction in spin splitting. More details about the nature of the chemical bonding can be found elsewhere [38,39].

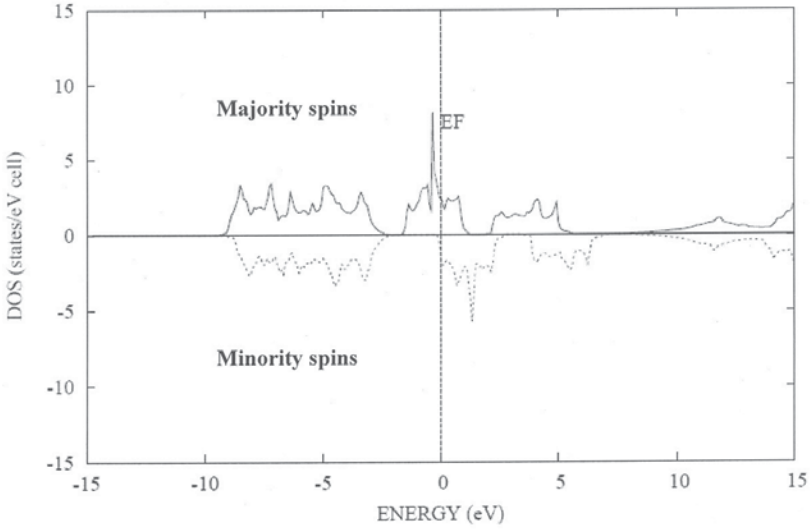

Fig. 13. Total (per formula unit) DOS for HMF CrO_2 at $P = 25.5$ GPa ($V/V_0 = 0.85$).

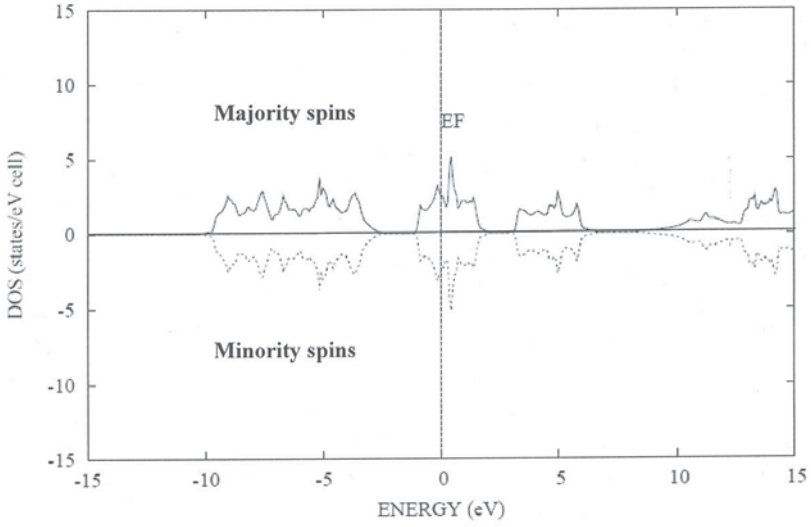

Fig. 14. Total (per formula unit) DOS for CrO_2 at $P = 41.6$ GPa ($V/V_0 = 0.80$).

In Figure 13 we have plotted total DOS at pressure of 25.5 GPa ($V/V_0 = 0.85$), where CrO_2 is still HM. The complete loss of HM occurs at a pressure of 41.6 GPa ($V/V_0 = 0.80$). At this pressure the DOS is plotted and given in Figure 14. Further increase in pressure kills magnetism and CrO_2 becomes non-magnetic at a pressure of 65 GPa.

As mentioned previously CrO_2 undergoes yet another transition to CaF_2-type from $CaCl_2$-type at 89.6 GPa. In Figures 15 and 16 we have plotted the BS and total DOS (for non-magnetic case), respectively for CaF_2-type structure. The lowest energy band near -20 eV corresponds to oxygen $2s$ states. Slight splitting in oxygen $2p$ states in broad band from -1 to -11 eV with small mixing of chromium $3d$ states can be seen in figures near Fermi level. The ground state properties of the present calculation are summarized in Table 1 along with the available results in literature.

4 Conclusion

From the present study we conclude that CrO_2, which crystallizes in rutile-type structure at ambient condition, undergoes two structural phase transitions namely tetragonal rutile-type to orthorhombic $CaCl_2$-type and $CaCl_2$-type to cubic CaF_2-type at 9.6 and 89.6 GPa, respectively. At ambient pressure CrO_2 is found to be stable in magnetic phase (ferromagnetic) and it also shows half metallicity with a saturated magnetic moment of $2\mu_B$/Cr. After it undergoes the first structural transition CrO_2 still remains as half metallic with a saturation magnetic moment of $1.833\mu_B$/Cr. Further increase in pressure quench half metallicity in CrO_2 at a pressure of 41.6 GPa. We predict another transition from $CaCl_2$- to CaF_2-type at pressure of 89.6 GPa, which can be experimentally verified. Apart from this, we also predicted that CrO_2 undergoes a second order magnetic to non magnetic transition at 65 GPa. The ground state properties are calculated and

Table 1. Ground state properties of CrO_2.

Properties		Rutile *P-I*	$CaCl_2$ *P-II*	CaF_2 *P-III*
Lattice parameter (Å)	Pre.	$a = 4.384$ $c = 2.889$	$a = 4.354$ $b = 4.249$ $c = 2.858$	$a = 4.334$
	Expt.	$a = 4.421$[a] $c = 2.916$[a]	–	–
Bulk modulus (GPa)	Pre.	143.3	193	338.2
$\mu(\mu_B/CrO_2)$	Pre.	2.0	1.833	0.0
	Expt.	2.0[b]	–	–
DOS (States/ eV. cell)	Pre.	2.30	2.93	5.07
	Others	0.69–2.35[a,c]	–	–
Structural transition pressure (GPa)	Pre.	9.6 (*P-I* → *P-II*)	89.6 (*P-II* → *P-III*)	
	Expt.	12.8[a]	–	
Magnetic transition (GPa)	Pre.	65 (FM→NM)		

Pre.→Present; Expt. → Experimental

[a] Reference [8]; [b] Reference [5]; [c] Reference [4].

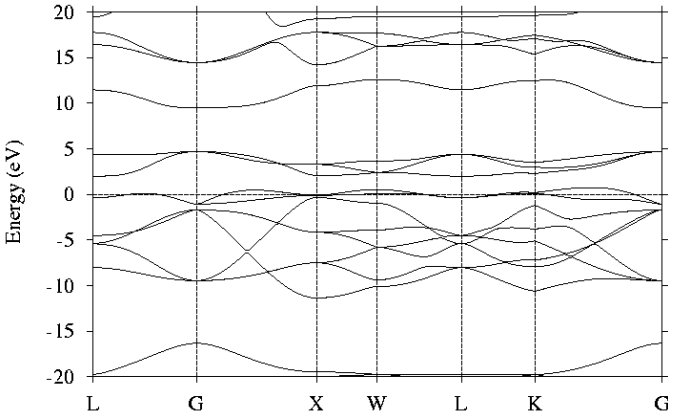

Fig. 15. Band structure for metallic non-magnetic CrO_2 at $P = 89.6$ GPa in CaF_2-type structure

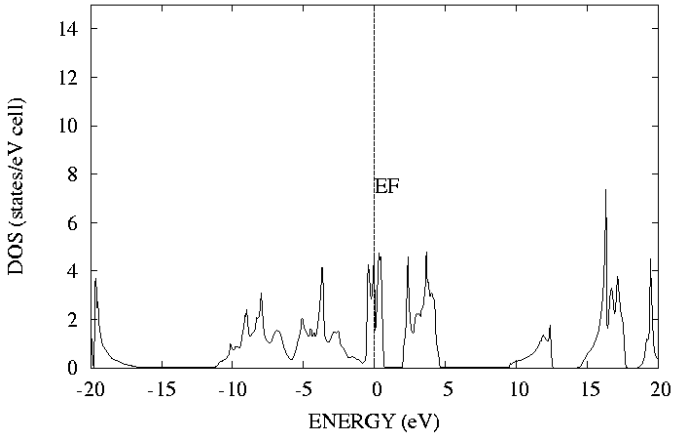

Fig. 16. Total (per formula unit) DOS for metallic non-magnetic CrO_2 at $P = 89.6$ GPa in CaF_2-type structure

presented in Table 1. The deviation between the calculated and experimental values may be due to the usage of LDA, which under estimate the lattice parameters and overestimate the bulk modulus. In addition, we have plotted the band structure and density of states. The bonding between Cr- and O- atoms is covalent in nature at ambient conditions. Under the application of pressure the compound starts losing the covalent bonding when half metallicity is quenched. When it becomes non magnetic CrO_2 becomes a metal. High-pressure experimental studies are indeed needed to verify our structural and magnetic properties of CrO_2.

VS is thankful to Department of Science & Technology (DST), New Delhi, India for the award of Young Scientist (DST project no. SR/FTP/PS-30/2005) under the Fast Track scheme and for financial support. SPS acknowledges Department of Atomic Energy (DAE), Mumbai for their partial financial support.

References

1. J.S. Moodera, L.R. Kinder, T.M. Wong, R. Meservey, Phys. Rev. Lett. **74**, 3273 (1995)
2. W.J. Gallagher et al., J. App. Phys. **81**, 3741 (1997)
3. H. Boeve, J.D. Boeck, G. Borghs, J. Appl. Phys. **89**, 482 (2001)
4. E. Kulatov, I.I. Mazin, J. Phys.: Condens. Matter **2**, 343 (1990)

5. S.P. Lewis, P.B. Allen, T. Sasaki, Phys. Rev. B **55**, 10253 (1997) and references therein
6. I.I. Mazin, D.J. Singh, C. Ambrosch-Draxl, Phys. Rev. B **59**, 411 (1999)
7. J.M.D. Coey, M. Venkatesan, J. Appl. Phys. **91**, 8345 (2002)
8. B.R. Maddox, C.S. Yoo, D. Kasinathan, W.E. Pickett, R.T. Scalettar, Phys. Rev. B **73**, 144111 (2006)
9. S.F. Matar, G. Demazeau, Chem. Phys. Lett. **407**, 516 (2005)
10. J. Haines, J.M. Léger, S. Hoyau, J. Phys. Chem. Solids **56**, 965 (1995)
11. S.S. Rosenblum, W.H. Weber, B.L. Chamberland, Phys. Rev. B **56**, 529 (1997)
12. K.J. Kingma, R.E. Cohen, R.J. Hemley, Ho-kwang Mao, Nature (London) **374**, 243 (1995)
13. S. Ono, K. Hirose, N. Nishiyama, M. Isshiki, Am. Mineral. **87**, 99 (2002)
14. L. Ranno, A. Barry, J.M.D. Coey, J. Appl. Phys. **81**, 5774 (1997)
15. K.H. Schwarz, J. Phys. F: Met. Phys. **16**, L211 (1986)
16. A.V. Nikolaev, B.V. Andreev, Phys. Solid State **35**, 603 (1993)
17. S. Matar, G. Demazeau, J. Sticht, V. Eyert, J. Kübler, J. Phys. I France **2**, 315 (1992)
18. M. Sicot, P. Turban, S. Andrieu, A. Tagliaferri, C. De Nadai, N.B. Brookes, F. Bertran, F. Fortuna, J. Magn. Magn. Mater. **303**, 54 (2006)
19. G.A. de Wijs, R.A. de Groot, Phys. Rev. B **64**, 020402 (2001)
20. R.S. Keizer, S.T.B. Goennenwein, T.M. Klapwijk, G. Miao, G. Xiao, A. Gupta, Nature **439**, 825 (2006)
21. Y. Ji, G.J. Strijkers, F.Y. Yang, C.L. Chien, J.M. Byers, A. Anguelouch, G. Xiao, A. Gupta, Phys. Rev Lett. **86**, 5585 (2001)
22. Yu. S. Dedkov, A.S. Vinogradov, M. Fonin, C. König, D.V. Vyalikh, A.B. Preobrajenski, S.A. Krasnikov, E. Yu. Kleimenov, M.A. Nesterov, U. Rüdiger, S.L. Molodtsov, G. Güntherodt, Phys. Rev. B **72**, 060401 (2005)
23. J.R. Patterson, C.M. Aracne, D.D. Jackson, V. Malba, S.T. Weir, P. A. Baker, Y.K. Vohra, Phys. Rev. B **69**, 220101 (2004)
24. A. Werner, H.D. Hochheimer, A. Jayaraman, J.M. Léger, Solid State Commun. **38**, 325 (1981)
25. A. Jayaraman, A.K. Singh, A. Chatterjee, S.U. Devi, Phys. Rev. B **9**, 2513 (1974)
26. R.E. Cohen, I.I. Mazin, D.G. Isaak, Science **275**, 654 (1997)
27. J. Haines, J.M. Léger, Phys. Rev. B **48**, 13344 (1993), and references therein
28. Dhrambir Singh, Vipul Srivastava, M. Rajagopalan, M. Husain, A.K. Bandyopadhyay, Phys. Rev. B **64**, 115110 (2001)
29. O.K. Andersen, Phys. Rev. B **12**, 3060 (1975)
30. O.K. Andersen, O. Jepsen, Phys. Rev. Lett. **53**, 2571 (1984)
31. W. Kohn, L.J. Sham, Phys. Rev. A **140**, 1133 (1965)
32. U. van Barth, L. Hedin, J. Phys. C **5**, 1629 (1972)
33. O. Jepsen, O.K. Andersen, Solid State Commun. **9**, 1763 (1971)
34. F. Birch, J. Geophys. Rev. **83**, 1257 (1978)
35. J. Kübler, A.R. William, C.B. Sommers, Phys. Rev. B **28**, 1745 (1983)
36. G. Prathiba, B. Anto Naanci, M. Rajagopalan, J. Mag. Mag. Mat. **309**, 251 (2007)
37. M.S. Miao, Walter R.L. Lambrecht, Phys. Rev. B **71** 64407 (2005)
38. P.I. Sorantin, K. Schwarz, Inorg. Chem. **31**, 567 (1992)
39. A. Yamanasi, L. Chioncel, A.I. Lichtenstein, O.K. Andersen, Phys. Rev. B **74**, 024419 (2006)